

Germanium hot-hole cyclotron-resonance maser with negative effective hole masses

A. A. Andronov, A. M. Belyantsev, V. I. Gavrilenko, E. P. Dodin, E. F. Krasil'nik,
V. V. Nikonorov, S. A. Pavlov, and M. M. Shvarts

Institute of Applied Physics, Academy of Sciences of the USSR

(Submitted 9 August 1985)

Zh. Eksp. Teor. Fiz. **90**, 367–384 (January 1986)

The physical principles underlying the occurrence of a population inversion and a negative differential conductivity of germanium hot holes at low temperatures in strong electric fields are set forth. Attention is focused on the conductivity of germanium hot holes at a cyclotron resonance in fields $\mathbf{H} \parallel \mathbf{E} \parallel [001]$. Under these conditions, stimulated emission has been achieved in the short-wave part of the millimeter wavelength range and in the submillimeter range. Experiments on the output characteristics of a germanium hot-hole cyclotron-resonance maser with negative effective hole masses are reported. The first experiments on the use of this maser for spectroscopic studies of semiconductors are also reported.

1. INTRODUCTION

Hot carriers (electrons and holes) in semiconductors have attracted considerable interest because of their possible use in active devices in solid-state microwave electronics, e.g., oscillators and amplifiers. Such hot-electron devices as IMPATT diodes and Gunn-effect devices have made it possible to extend active systems of solid-state microwave electronics to wavelengths as short as $\lambda \sim 1$ mm. Recent experiments^{1–5} indicate that it will be possible to develop hot-carrier devices for even shorter wavelengths, into the mid-IR range. Such devices would operate by virtue of the negative differential volume conductivity of hot carriers in semiconductors, which arises from a population inversion of carriers in strong electric and magnetic fields. In the present paper we discuss the physical principles underlying the operation of one such device, a germanium hot-hole cyclotron-resonance maser with negative effective hole masses. We also report theoretical and experimental studies of this maser.

Although a negative effective mass amplifier and generator (NEMAG) based on the charge carriers (holes) in *p*-type semiconductors were suggested by Krömer⁶ back in 1958, it was not until 1984 that lasing was actually achieved.⁴ Despite this delay of more than a quarter of a century in actual implementation in a device, the NEMAG idea has done much to stimulate research on hot carriers and a search for conditions for achieving a negative differential conductivity in semiconductors (see, for example, the review in Ref. 7). After the lapse of so many years we can only speculate on why the work on NEMAG was essentially halted back in the mid-1960s. The most likely reason is that Krömer's suggestion was not sufficiently specific. The role played by the population inversion of holes in the appearance of a negative differential conductivity was not fully understood, although the need for an inversion for a negative differential conductivity in NEMAG was pointed out.^{8,9} At the time, no detailed calculations had been carried out on the distributions and conductivity of hot holes. The conditions for achieving an inversion in the hole distribution and for

achieving a negative differential conductivity were thus not completely clear. In fact, there was point of view⁸ which held that an inversion could not occur in the distribution of hot carriers.

Interest in NEMAG revived as a result of the progress achieved over the past 7–10 years toward an understanding of the conditions for the occurrence of an inversion in the distribution of hot carriers and the possible use of this inversion in active systems. In the present paper we will focus on the cyclotron version of NEMAG in $\mathbf{E} \parallel \mathbf{H}$ fields; this version has been realized in practice. For a complete picture, however, we will also theoretically examine the original version of NEMAG, without a magnetic field.

2. NEGATIVE DIFFERENTIAL CONDUCTIVITY IN A STRONG ELECTRIC FIELD WITH $\mathbf{E} \parallel [001]$

Krömer's idea⁶ was to use a *p*-type semiconductor (*p*-Ge, *p*-Si, etc.) to generate and amplify electromagnetic oscillations. In the semiconductor, the degeneracy of the valence bands would make the dispersion for heavy holes anisotropic, so that there would be certain directions along which the transverse effective mass of the holes would be negative. In momentum space, the regions of negative effective masses are cones along [001] axes or rings with a corrugated surface formed when such cones coalesce¹⁾ (Refs. 6 and 10). If a field E_1 is applied to the semiconductor in a direction along which the effective mass of some of the holes is negative, the current j of the holes will slow in the direction opposite the field; the field will perform negative work on the holes:

$$\Delta j_i = e \Delta v_i = e \Delta \frac{\partial \epsilon}{\partial p_i} = e \frac{\partial^2 \epsilon}{\partial p_i^2} \Delta p_i = e^2 \frac{\partial^2 \epsilon}{\partial p_i^2} E_{1i} \Delta t, \quad (1)$$

$$\Delta P = \Delta j_i E_{1i} = e^2 (E_{1i})^2 \Delta t \frac{\partial^2 \epsilon}{\partial p_i^2} < 0 \quad \text{for} \quad \frac{1}{m_{ii}^{(1)}} \equiv \frac{\partial^2 \epsilon}{\partial p_i^2} < 0. \quad (2)$$

Here ϵ , v , and p are the energy, velocity, and quasimomentum of the holes. Figure 1a shows the intersection of the constant-energy surface of the Ge heavy holes,

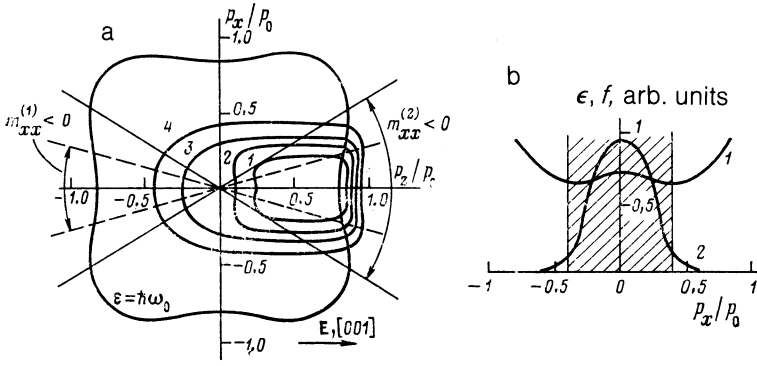


FIG. 1. a: Regions of a negative effective mass, $m_{xx}^{(1,2)}$, in the $p_y = 0$ plane in momentum space and contour lines of a uniform distribution of germanium heavy holes during streaming in a static field $E \approx 120$ V/cm (Ref. 21). f_0 (arbitrary units): 1—0.8; 2—0.6; 3—0.2; 4—0.1. b: The energy ε (1) and the distribution function f (2) during the streaming of Ge heavy holes versus the transverse momentum ($E = 120$ V/cm, $p_z/p_0 = 0.7$, $p_y = 0$). The hatched region is the region of an inversion of the distribution function, with $\partial f/\partial \varepsilon > 0$.

$\varepsilon(p) = \text{const}$, with the plane $p_y = 0$ in momentum space. The dashed lines are the boundaries of the region of negative effective masses, $m_{xx}^{(1)} < 0$. It follows from (1) and (2) that one hole in this region is capable of strengthening the field E_x ($\Delta P < 0$), while the overall effect of the interaction of all the holes with the field (absorption or amplification) depends on the nature of the distribution function of the holes. A necessary condition for the existence of a negative differential conductivity is an inversion of the distribution function along the direction of the field E_1 : $(\partial f/\partial \varepsilon)_{\parallel E} > 0$ (Refs. 7–9, for example). Such an inversion can be set up by a strong static electric field E . In this case, as we will show below, an anisotropic distribution function, stretched out along E , as shown in Fig. 1a, is formed in a semiconductor at temperatures below the Debye temperature, $k_B T \ll \hbar\omega_0$ ($\hbar\omega_0$ is the energy of an optical phonon). With a suitable crystallographic orientation of E , e.g., $E \parallel [001]$ (as in Fig. 1a), a function of this sort is inverted in the direction transverse with respect to E by virtue of the anisotropy of the heavy-hole dispersion. This situation can be seen in Fig. 1b, which shows ε and f as functions of p_x in one of the cross sections $p_z = \text{const} \neq 0$, $p_y = 0$. Since the constant-energy surface of the heavy holes is concave along the $[001]$ direction, the dependence of ε on p_x is not monotonic, and for the given type of distribution function, decreasing with distance from the p_z axis, we have

$$(\partial f/\partial \varepsilon)_{p_y=0, p_z=\text{const}} > 0$$

in the region where we have

$$1/m_{xx}^{(2)} = (1/p_x) (\partial \varepsilon/\partial p_x) < 0$$

(in the region bounded by the solid lines in Fig. 1a).

An expression for the transverse conductivity of the holes can be found by solving the kinetic equation for the distribution function in the resultant electric field $E + E_1$ ($E \parallel [001]$, $E_1 \perp E$). In the case of a weak alternating field $E_1 \propto e^{i\omega t}$ ($E_1 \ll E$), the distribution function can be represented as the sum of a steady-state distribution formed by the strong static field E and an oscillating part: $f = f_0 + f_1$. In this case the equation for f_1 takes the following form in the τ approximation:

$$\frac{\partial f_1}{\partial t} + eE \frac{\partial f_1}{\partial p_x} = -\nu f_1 - eE_1 \frac{\partial f_0}{\partial p} \quad (3)$$

Integrating (3) with the boundary condition $f_1(p_z = -\infty) = 0$, we find f_1 and the differential hole conductivity σ_{ij} :

$$\sigma_{ij} = \frac{eN_0}{E_{ij}} \iiint \frac{\partial \varepsilon}{\partial p_i} f_1 dp_x dp_y dp_z = -\frac{e^2 N_0}{\omega_E p_0} \iiint dp_x dp_y dp_z \times \exp\left(-\frac{i\omega + \bar{\nu}}{\omega_E} \frac{p_z}{p_0}\right) \frac{\partial \varepsilon}{\partial p_i} \int_{-\infty}^{p_z} \exp\left(\frac{i\omega + \bar{\nu}'}{\omega_E} \frac{p_z'}{p_0}\right) \frac{\partial f_0(p')}{\partial p_j} dp_z' \quad (4)$$

Here $\mathbf{p}' = i p_x + \mathbf{j} p_y + \mathbf{k} p_z'$, $\omega_E = eE/p_0$, p_0 is the average momentum of a hole with an energy $\hbar\omega_0$, $\nu(p)$ is the momentum relaxation rate, and

$$\bar{\nu} = \frac{1}{p_z} \int \nu(p) dp_z, \quad \bar{\nu}' = \bar{\nu}(p').$$

Since the $[001]$ crystallographic direction, along which the static electric field E is applied, is a fourfold symmetry axis, the linear transverse conductivity is isotropic, and we have $\sigma_{xx} = \sigma_{yy}$, $\sigma_{xy} = \sigma_{yx} = 0$.

The absorbed power is determined by the real part of expression (4) for σ_{xx} . At low frequencies, $\omega \ll \bar{\nu}$, ω_E , the induced current \mathbf{j}_1 is in phase with the field E_1 , and we have $\text{Im} \sigma_{xx} = 0$. For a steady-state distribution function f_0 which falls off with distance from the p_z axis, a negative contribution is made to the conductivity by those holes for which the condition $(\partial \varepsilon/\partial p_x)(\partial f/\partial p_x) > 0$ holds, according to (4). These are holes which are localized in a region of momentum space corresponding to $\varepsilon < \hbar\omega_0$, where we have $m_{xx}^{(2)} < 0$ (Fig. 1). This region is broader than that in which the condition $m_{xx}^{(1)} < 0$ holds, as was pointed out by Krömer, who used expressions similar to (1) and (2) (several other investigators have subsequently mentioned the same point). Krömer was discussing the idea of NEMAG using germanium heavy holes in a strong electric field E (Refs. 6 and 10).

At high frequencies, $\omega \gtrsim \omega_E, \omega \gg \bar{\nu}$, the function $\text{Re} \sigma_{xx}(\omega)$ is oscillatory and the absolute value $|\text{Re} \sigma_{xx}|$ falls off roughly in accordance with $(\omega/\omega_E)^{-2}$ (Ref. 11, for example). For a needle-shaped distribution function, elongated along the p_z axis, we have $\text{Re} \sigma_{xx} \leq 0$ at all frequencies. For a finite width f_0 in the direction transverse with respect to E , regions of negative and positive conductivity alternate, as is shown by the calculations (Fig. 2).

An anisotropic distribution function, elongated along

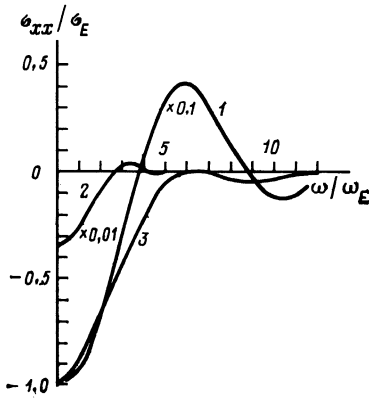


FIG. 2. Real part of the transverse conductivity σ_{xx} of germanium heavy holes at (1) $T = 12$ K and (2) 24 K in a field with $\mathbf{E} \parallel [001]$, $E = 150$ V/cm, according to a numerical simulation of the distribution function by the Monte Carlo method. Also shown (3) is the conductivity σ_{xx} of holes with a needle-shaped distribution function ($f_0 = A\delta(p_x)\delta(p_y)$, $0 < p_z < p_0$); $\sigma_E = e^2 N_0 / \bar{m} \omega_E$, $\bar{m} = 0.3 m_0$.

the field \mathbf{E} , arises in moderately doped p -type Ge at low temperatures, $k_B T \ll \hbar \omega_0$, under the conditions $\nu < \omega_E < \nu_0$, where ν and ν_0 are typical values of the hole scattering rate at $\varepsilon < \hbar \omega_0$ and $\varepsilon > \hbar \omega_0$, respectively. The holes are accelerated essentially without scattering in the electric field up to an energy $\varepsilon = \hbar \omega_0$; they emit an optical phonon; they return to the low-energy region; they reacquire an energy $\hbar \omega_0$; etc. The result is an anisotropic distribution of holes in momentum space, stretched out along the E direction, i.e., streaming.¹²⁻¹³ It is the localization of this distribution in the region of negative effective masses, $m_{xx}^{(2)} < 0$ (this region is broader than the region $m_{xx}^{(1)} < 0$ considered by Krömer), which leads to the inversion in the hole distribution, as has been shown.

It is a rather complicated problem to find the distribution function f_0 under streaming conditions. The most complete information here can be found through numerical simulation by the Monte Carlo method (Refs. 13 and 14, for example). The distribution function was first calculated by this method assuming an isotropic dispersion of heavy holes in germanium.¹³ Estimates of the anisotropy of the conductivity based on those calculations showed that for $\mathbf{E} \parallel [001]$ a negative differential conductivity occurs at $T \lesssim 7$ K at static fields in the range 50–100 V/cm. Unfortunately, the quantitative nature of these results rules out any conclusions regarding the actual values of the conductivity, its frequency dependence, or the temperature limits on the existence of a negative differential conductivity.

In the present study the distribution function f_0 is simulated by the Monte Carlo method for the actual heavy-hole dispersion law; scattering by acoustic and optical phonons is taken into account (see also Section 4). The results are used with expression (4) to find the transverse conductivity. Figure 2 shows some typical results on the behavior $\sigma(\omega)$. The absolute value of the conductivity reaches a maximum at low frequencies. At $T = 12$ K, it is an order of magnitude lower²⁾ than the value for a needle-shaped distribution function localized at the p_z axis at $0 < p_z < p_0$ (cf. Ref. 11). At $T = 24$ K,

the conductivity at these frequencies decreases even further, by more than an order of magnitude. These results show that the negative differential conductivity is actually the difference between two approximately equal components of the conductivity, from the inverted and noninverted parts of the distribution function. As a result, a slight decrease in the inverted part (as we go from $T = 12$ K to $T = 24$ K) produces a sharp decrease in the negative differential conductivity, to the point where it vanishes at³⁾ $T \sim 30$ K. Impurity scattering (ignored in the numerical simulation in the present study), even in samples with a low doping level, $p \gtrsim 10^{13}$ cm⁻³, could play a similar role in the decrease and disappearance of the negative differential conductivity. In light of all these factors, we see why Krömer's idea of a universal negative-mass generator and amplifier for a broad frequency range remained unrealized as long as it did.

3. LINEAR CONDUCTIVITY OF GERMANIUM HEAVY HOLES AT A CYCLOTRON RESONANCE IN FIELDS WITH $\mathbf{E} \parallel \mathbf{H} \parallel [001]$

The magnitude of the negative differential conductivity of a p -Ge in a strong electric field with $\mathbf{E} \parallel [001]$ can be increased substantially at frequencies above 10^{11} Hz under cyclotron resonance conditions for holes with a negative effective mass in a magnetic field^{6,18} such that $\mathbf{H} \parallel \mathbf{E} \parallel [001]$. The cyclotron mass m_c of germanium heavy holes [$m_c = (2\pi)^{-1} \partial S / \partial \varepsilon$, S is the area bounded by the cyclotron orbit], like the effective transverse mass, can take on negative values in certain regions in momentum space, specifically, two cones, symmetric with respect to the $p_z = 0$ plane, with axes along \mathbf{H} and with vertices at the point $p = 0$. The boundaries of the negative-cyclotron-mass cones in the $p_y = 0$ plane coincide with the boundaries of the region $m_{xx}^{(2)} < 0$ (Fig. 1a). The surfaces of constant cyclotron frequency $\omega_c = eH/m_c c$ of holes with a negative cyclotron mass are also conical, with axis along \mathbf{H} and with vertex at $p = 0$. The cyclotron frequency varies from zero at the boundary of the negative-cyclotron-mass cone to $\omega_c / \omega_{c0} = A - (B^2 + \frac{1}{2}C^2)/B \approx -4.27$ at the p_x axis. Here $\omega_{c0} = eH/m_0 c$; m_0 is the mass of a free electron; and $A = 13.27$, $B^2 = 74.48$, and $C^2 = 153.8$ are constants which appear in the dispersion law for the heavy holes¹⁰:

$$\varepsilon = \frac{1}{2m_0} \{ A p^2 - [B^2 p^4 + C^2 (p_x^2 p_y^2 + p_y^2 p_z^2 + p_z^2 p_x^2)]^{\frac{1}{2}} \}.$$

In a magnetic field such that $\mathbf{H} \parallel [001]$, holes with a negative cyclotron mass gyrate the way electrons would in free space—in the direction opposite that in which ordinary holes would revolve. Consequently, the cyclotron resonance of holes with a negative cyclotron mass will prevail for a wave of circular polarization in the “electron direction,” propagating along \mathbf{H} . For holes with positive cyclotron masses, the resonant wave would be a wave with an opposite, “hole,” circular polarization. In thermodynamic equilibrium the fraction of heavy holes with a negative cyclotron mass is about 7% (Ref. 19), and they are not important in the conductivity. The situation changes dramatically when there is an inversion in a strong electric field $\mathbf{E} \parallel [001]$. The imposition of a magnetic field with $\mathbf{H} \parallel \mathbf{E}$ makes it possible

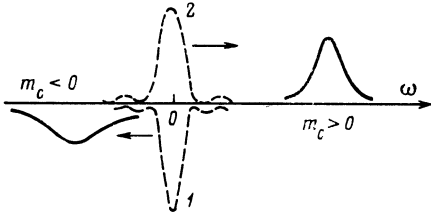


FIG. 3. Frequency dependence of the real part of the transverse conductivity of Ge heavy holes from the (1) inverted and (2) noninverted regions of the distribution function under streaming conditions (schematic) representation. Dashed line— $H = 0$; solid line—cyclotron resonance for a circularly polarized alternating electric field $\mathbf{E}_1 \perp \mathbf{H} \parallel \mathbf{E}$.

under cyclotron resonance conditions ($\omega_c \gg \omega_E, \nu$) to distinguish the components of the conductivity due to the inverted and noninverted parts of the distribution function (Fig. 3), i.e., of holes with negative and positive cyclotron masses. The magnitude of the negative differential conductivity in an alternating electric field with a circular polarization in the electron direction becomes significantly larger in this case than in the case $H = 0$. Although the first calculations of the conductivity under such conditions were carried out in Ref. 20, the *a priori* specification of a heavy-hole distribution function detracted significantly from the results; judging from the literature, that study did not stimulate further research. It was not until some twenty years later that the idea of streaming in *p*-Ge, which had been developed by that time, was used in Ref. 21 to demonstrate the existence of a negative differential conductivity at cyclotron resonance; the limiting values of E, H, T , and ω were calculated, facilitating a subsequent search for the conditions for the appearance of stimulated emission.⁴ As in the case $H = 0$, an expression for the linear conductivity of holes at cyclotron resonance in fields with $\mathbf{H} \parallel \mathbf{E} \parallel [001]$ can be found analytically by solving the kinetic equation for the oscillatory part of the distribution function, f_1 . To find the steady-state part of the distribution function f_0 is even more difficult than at $H = 0$, and this can be done for the actual dispersion law only through numerical simulation. An analytic solution was derived in Ref. 21 through the approximation of a dispersion law which was axisymmetric around the p_z axis. That law leads to a good description of the dynamics of holes with a negative cyclotron mass, and such holes make a resonant contribution to the conductivity at cyclotron resonance. Because of the symmetry of the problem, a magnetic field $\mathbf{H} \parallel \mathbf{E} \parallel [001]$ does not affect the steady-state part of the distribution function, so that the kinetic equation for f_0 can be solved at $H = 0$. Figure 1a shows $f_0(p_x, p_z) = \text{const}$ contour lines of the distribution function found by this approach. The maximum value of f_0 is reached near the p_z axis, but not at the axis itself, as it would be in the case of an isotropic dispersion law.¹³ The dip in the function f_0 at the axis is very slight (a few percent)²¹; that region is omitted from Figs. 1a and 1b.

To find the oscillatory part of the distribution function in a strong magnetic field $\omega_c \gg \omega_E$, it is convenient to switch from the variables p_x, p_y in the kinetic equation to new canonical variables, the angle φ and the action S . In this case

these variables are, respectively, the phase of the motion of a hole along its cyclotron orbit and the area of this orbit:

$$\begin{aligned} \dot{p}_x &= \frac{\partial \mathcal{H}}{\partial p_y}, & \dot{p}_y &= -\frac{\partial \mathcal{H}}{\partial p_x}, \\ \dot{\varphi} &= \frac{\partial \mathcal{H}}{\partial S} = \omega_c(S, p_z), & \dot{S} &= -\frac{\partial \mathcal{H}}{\partial \varphi} = 0, \end{aligned} \quad (5)$$

$$\dot{p}_z = eE,$$

where $\mathcal{H} = e\mathbf{E}H/c$. In terms of these new variables, the kinetic equation for f_1 becomes

$$\frac{\partial f_1}{\partial t} + \omega_c \frac{\partial f_1}{\partial \varphi} + eE \frac{\partial f_1}{\partial p_z} = -\frac{e^2 H}{\omega_c c} \mathbf{E}_1 \mathbf{v} \frac{\partial f_0}{\partial S} - \nu f_1. \quad (6)$$

Here $\mathbf{v} = \partial \mathcal{E} / \partial \mathbf{p}$ is the velocity of the hole. The right side of this equation is a resonant force for f_1 at frequencies $\omega = n\omega_c$. Since the revolution of holes with a negative cyclotron mass far from the boundary of the cone $\omega_c(p) = 0$ is largely harmonic (Ref. 19, for example), we restrict the discussion to cyclotron resonance at the fundamental frequency. For the first harmonic of the revolution velocity of holes with a negative cyclotron mass, $V_1(S, p_z) e^{i\varphi}$ ($\varphi = \omega_c t + \varphi_0$), the resonant electric field is a field \mathbf{E}_1 of circular polarization in the electron direction: $\mathbf{E}_1 \sim e^{i\omega t}$. Solving Eq. (6) by analogy with Ref. 21, and considering the contribution to the conductivity only from holes which are in resonance with the field $\mathbf{E}_1(\omega)$, which lie near the cone $\omega = -\omega_c(S, p_z)$, we find $\sigma(\omega)$. The real part of this conductivity is given in the limit⁴ $\omega_E, \nu \rightarrow 0$ by

$$\begin{aligned} \text{Re } \sigma &= \sigma_{\text{res}} = -2\pi^2 e^2 \iint \{ dp_x dp_y dS \delta(\omega - \omega_c(S, p_z)) \} |V_1|^2 \\ &\times \left(\frac{\partial f_0}{\partial \mathbf{E}} \right)_{1 \perp \hat{p}_z} = -2\pi^2 e^2 \iint dS \left\{ |V_1|^2 \left(\frac{\partial f_0}{\partial \mathbf{E}} \right)_{1 \perp \hat{p}_z} \right. \\ &\quad \left. \times \left| \frac{\partial \omega_c(S, p_z)}{\partial p_z} \right|^{-1} \right\}_{\omega = -\omega_c(S, p_z)} \end{aligned} \quad (7)$$

The integration over dS here is carried out over the surfaces of both of the resonant cones, over the entire energy range, $\mathcal{E}(\mathbf{p}) \leq \hbar\omega_0$; the derivative $\partial f_0(S, p_z) / \partial \mathbf{E}$ is calculated in the direction perpendicular to the p_z axis. It follows from expression (7) that the negative component of the conductivity at the frequency ω comes from holes which are in this part of momentum space on the resonant cone $\omega_c(S, p_z) = -\omega$, where the distribution function is inverted: $(\partial f_0 / \partial \mathbf{E})_{1 \perp p_z} > 0$. Figure 4 shows the function $\sigma_{\text{res}}(\omega)$ for certain values of the static electric field E . These curves were found by integrating (7), assuming an axisymmetric dispersion law, for the steady-state distribution function f_0 calculated for this model.²¹ The nonresonant transverse conductivity of holes in fields such that $\mathbf{E} \parallel \mathbf{H}$ can be calculated from²²

$$\sigma_h = \frac{e^2 N_0}{\bar{m}} \frac{\omega_E}{(\omega + \bar{\omega}_c)^2} \left(1 + \frac{\Gamma(5/3) \Gamma(1/3)}{6} \right) \approx \frac{e^2 N_0}{\bar{m}} \frac{1.4 \omega_E}{(\omega + \bar{\omega}_c)^2}, \quad (8)$$

where $\bar{m} = 0.32m_0$, $\bar{\omega}_c = eH/\bar{m}c$, and Γ is the gamma function. Comparing σ_h and σ_{res} (Fig. 4), we find

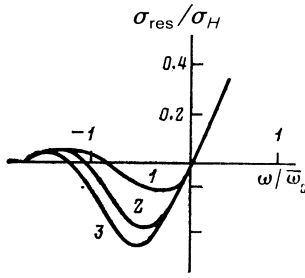


FIG. 4. Real part of the resonant conductivity σ_{res} of hot heavy holes in germanium with a negative cyclotron mass ($\omega/\omega_c < 0$). E (V/cm): 1—480; 2—240; 3—120; $\sigma_H = e^2 N_0 / m \bar{\omega}_c$.

$\sigma_\Sigma = \sigma_{res} + \sigma_h < 0$ at frequencies $\omega > \omega_E$. At liquid-helium temperature, the streaming of heavy holes ($\omega_E \gtrsim \nu$) arises at fields¹³ $E \gtrsim 100$ V/cm, corresponding to a transit frequency $\omega_E \approx 3 \cdot 10^{10}$ s⁻¹ which actually determines the long-wave boundary of the region of negative differential conductivity. The short-wave boundary is determined by the quantization of the energy spectrum of the heavy holes. At energies $\varepsilon < \hbar\omega_0$, no fewer than two Landau levels should fall within the negative-cyclotron-mass cone. This requirement leads to the condition $\omega < 10^{13}$ s⁻¹ ($\lambda > 0.2$ mm).

Numerical estimates for $\omega = 10^{12}$ s⁻¹, $E = 120$ V/cm, $H = 25$ kOe, and $N_0 = 10^{14}$ cm⁻³ yield $\sigma_{res} \approx 2 \cdot 10^{10}$ s⁻¹, and $\sigma_h \approx 5 \cdot 10^8$ s⁻¹. The corresponding gain is

$$\alpha = k_0 n'' = (\omega/c) \operatorname{Im}[\varepsilon_0 - i(4\pi\sigma_\Sigma/\omega)]^{1/2} \approx 1 \text{ cm}^{-1}.$$

4. NEGATIVE DIFFERENTIAL CONDUCTIVITY IN A STRONG ALTERNATING ELECTRIC FIELD

The negative differential conductivity of *p*-Ge in strong static fields with $\mathbf{E} \parallel \mathbf{H}$ can lead to such a substantial intensification of a weak alternating electric field $\mathbf{E}_1(\omega)$, either resulting from fluctuations or the field of an electromagnetic wave incident on the semiconductor from the exterior, that the conductivity $\sigma(\omega)$ changes. It is not possible to derive an analytic expression for the heavy-hole conductivity from the solution of the kinetic equation in the case of an arbitrary field amplitude E_1 . An effective method here is a numerical simulation of the conductivity; we report the results of such a simulation below. Certain qualitative conclusions regarding the nature of the hole conductivity in a circularly polarized strong field E_1 can be extracted from a direct analysis of the equations of motion in fields $\mathbf{E}_1 \perp \mathbf{E} \parallel \mathbf{H}$:

$$\begin{aligned} \dot{p} &= eE \cos \theta + eE_1 \sin \theta \cos \varphi + \frac{eH}{c} \frac{1}{p} \frac{\partial \varepsilon}{\partial \varphi}, \\ \dot{\Phi} &= \omega + \frac{eH}{c} \frac{1}{p} \left(\frac{\partial \varepsilon}{\partial p} + \operatorname{ctg} \theta \frac{1}{p} \frac{\partial \varepsilon}{\partial \theta} \right) - \frac{eE_1}{p \sin \theta} \sin \Phi, \\ \dot{\theta} &= \frac{eE_1}{p} \cos \theta \cos \Phi - \frac{eE}{p} \sin \theta + \frac{eH}{c} \frac{1}{p^2} \operatorname{ctg} \theta \frac{\partial \varepsilon}{\partial \varphi}. \end{aligned} \quad (9)$$

Equations (9) are written in terms of the polar coordinates

$$\Phi = \omega t - \varphi, \quad \mathbf{E}_1 = E_1 (\mathbf{i} \cos \omega t + \mathbf{j} \sin \omega t).$$

As the holes drift and revolve in the $\mathbf{E} \parallel \mathbf{H}$ fields, they intersect the cone $\omega_c(\mathbf{p}) = -\omega$, near which their interac-

tion with the field E_1 is resonant. In a strong alternating field, the holes can exhibit autoresonant behavior; as they are "uncoiled" by the field E_1 , they are captured to the resonant cone and do not leave resonance until the next scattering event. In Ref. 23 a model of an axisymmetric heavy-hole dispersion law,

$$\varepsilon(\mathbf{p}) = (p^2/2m) (1 + \xi \cos 4\theta),$$

was used, and it was shown that system of equations (9) has a solution in the form of a rotational translational motion along the surface of the resonant cone:

$$\omega_c(\theta_0) = \frac{eH}{c} \left(\frac{1}{p} \frac{\partial \varepsilon}{\partial p} + \frac{1}{p^2} \frac{\partial \varepsilon}{\partial \theta} \operatorname{ctg} \theta \right)_{\theta=\theta_0} = -\omega:$$

$$\theta = \theta_0 = \text{const}, \quad \varphi = -\omega_c t, \quad p = \frac{eE_1 t}{\sin \theta_0} \quad \text{for} \quad \frac{E_1}{E} = \operatorname{tg} \theta_0. \quad (10)$$

Solution (10) is stable with respect to small perturbations of θ and φ ; i.e., near the resonant cone in momentum space there is a region in which, once a hole enters, the hole becomes captured to the cone and subsequently moves along its surface.⁵⁾ The power absorbed in the process,

$$P = \mathbf{j} \cdot \mathbf{E}_1 = e^2 E_1^2 t / m_c,$$

is negative if $m_c < 0$, and it increases in magnitude in proportion to the time of free flight between scattering events.

Figure 5 shows a numerical solution of Eqs. (9) in a strong alternating field E_1 which is circularly polarized in the electron direction for the actual dispersion law of Ge heavy holes. A hole which has been captured to the resonant cone moves along an uncoiling spiral; its absorption is negative and increases in absolute value in proportion to t , while the absorption of the uncaptured holes oscillates around zero. A numerical solution of the equations of motions of holes with various initial conditions shows that under the condition $\omega_c \gg \omega_E$ the captured holes constitute a significant fraction of the total number of holes.²³ In a strong field E_1 , the hole may therefore bunch near a resonant cone, and the absolute value of the negative differential conductivity can increase.

The conductivity σ was studied as a function of the strength of the alternating field E_1 through a Monte Carlo numerical simulation which took into account both the particular features of the dynamics of holes with a complex dispersion law and the scattering in the strong fields \mathbf{E}_1 , \mathbf{E} , and \mathbf{H} . The equations of motions were integrated, and the velocity $\mathbf{v}(t)$, the current $\mathbf{j}(t)$, and the average absorbed power⁶⁾

$$\bar{P} = \lim_{N \rightarrow \infty} \left\{ \frac{1}{T} \sum_{k=0}^{N-1} \int_{\tau_k}^{\tau_{k+1}} \mathbf{j}(t) \cdot \mathbf{E}_1(t) dt \right\}$$

were calculated. Here N is the number of scattering events, and (τ_k, τ_{k+1}) is the interval between the k th and $(k+1)$ st events. The calculations incorporate the scattering of holes involving the emission and absorption of acoustic and optical phonons. The corresponding probability densities for a transition of a hole from state \mathbf{p} to state \mathbf{p}' per unit time are (Ref. 14, for example)

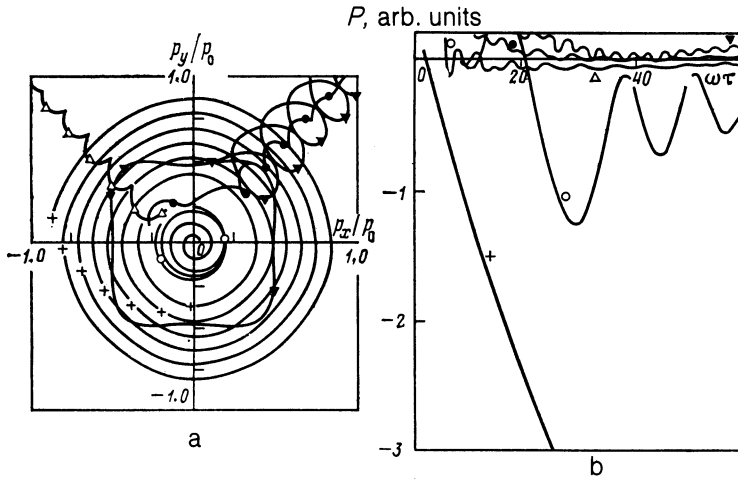


FIG. 5. a: Rotational-translational motion of holes in fields $E_1 \perp E \parallel H \parallel \hat{p}_z \parallel [001]$ (projections of the paths onto the $p_z = 0$ plane are shown here). The field E_1 is resonant with holes having a negative cyclotron mass [see (10)]. Markers on the paths show equal time intervals Δt , corresponding to the motion of a hole a distance $\Delta p_z = eE\Delta t$ along p_z . b: Absorption of a circularly polarized electromagnetic wave E_1 by various holes (the markers have the same meaning as in part a). The curve with the plus sign corresponds to the absorption of a hole with a negative cyclotron mass which has been captured to the resonant cone $\omega_c(\mathbf{p}) = -\omega$.

$$W_{ac} = \frac{2\pi}{\hbar^2} B_{ac} |\mathbf{p} - \mathbf{p}'| \left\{ \frac{N_q}{N_q + 1} \right\} \delta(\varepsilon(\mathbf{p}') - \varepsilon(\mathbf{p})), \quad (11)$$

$$W_{opt} = \frac{2\pi}{\hbar} B_{opt} \left\{ \frac{N_0}{N_0 + 1} \right\} \delta(\varepsilon(\mathbf{p}') - \varepsilon(\mathbf{p}) \mp \hbar\omega_0), \quad (12)$$

where

$$B_{ac} = \hbar E_{1s}^2 / 4\rho V_0 s, \quad B_{opt} = \hbar (D_i K)^2 / 2\rho V_0 \omega_0,$$

and $N_{q,0} = \{\exp(\hbar\omega_{q,0}/k_B T) - 1\}^{-1}$ is the phonon distribution according to Bose-Einstein statistics. Here V_0 is the crystal volume, $E_{1s} = 4.6$ eV is the constant of the acoustic interaction,⁷⁾ $D_i K = 9 \cdot 10^8$ eV/cm is the constant of the strain energy, $\rho = 5.32$ g/cm³ is the density of the crystal, $s = 4 \cdot 10^5$ cm/s is the sound velocity, and $\hbar\omega_0 = 0.037$ eV is the energy of an optical phonon. Expressions (11) and (12) can be used to determine the integrated probabilities for the transitions of particles out of the state \mathbf{p} ; these probabilities are used to determine the scattering mechanism in each scattering event during the simulation. For an interaction with uniformly distributed acoustic phonons⁸⁾ the integrated

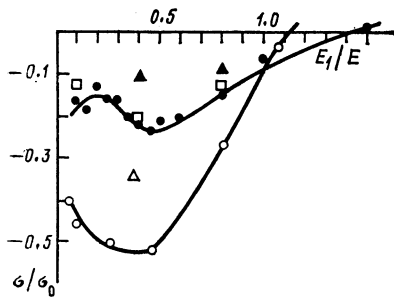


FIG. 6. Real part of the conductivity at cyclotron resonance of germanium heavy holes in fields such that $E \parallel H \parallel [001]$ according to a Monte Carlo numerical simulation for the following values of E, H, ω (E_1 is the circularly polarized field which is in resonance with the holes with the negative cyclotron mass; $T = 24$ K): \bullet — $E = 200$ V/cm, $H = 34$ kOe, $\omega = 10^{12}$ s⁻¹; \square — 200 V/cm, 69 kOe, $2 \cdot 10^{12}$ s⁻¹; \blacktriangle — 200 V/cm, 136 kOe, $4 \cdot 10^{12}$ s⁻¹; Δ — 200 V/cm, 25 kOe, 10^{12} s⁻¹; \circ — 150 V/cm, 25 kOe, 10^{12} s⁻¹.

scattering probabilities are

$$\begin{aligned} v_{ac}^{\mp} &= \frac{1}{4\sqrt{2}} \frac{E_{1s}^2 k_B T m_{ds}^{3/2} \varepsilon^{3/2}}{\pi \hbar^4 \rho s^2} \\ &= 0.54 \cdot 10^8 T [\text{K}] \{(\varepsilon/k_B) [\text{K}]\}^{3/2} [\text{s}^{-1}], \end{aligned}$$

while for the interaction with optical phonons they are

$$\begin{aligned} v_{opt}^{\mp} &= \frac{1}{\sqrt{2}} \frac{(D_i K)^2 m_{ds}^{3/2}}{\pi \rho \hbar (\hbar\omega_0)^{3/2}} \left\{ \frac{N_0}{N_0 + 1} \right\} \left\{ \frac{\varepsilon}{\hbar\omega_0} \pm 1 \right\}^{1/2} \\ &\approx 2v_0 \left\{ \frac{N_0}{N_0 + 1} \right\} \left(\frac{\varepsilon}{\hbar\omega_0} \pm 1 \right)^{1/2}, \end{aligned}$$

where

$$m_{ds}^{3/2} = \frac{m_0^{3/2}}{4\pi} \int_0^{2\pi} \int_0^{\pi} \frac{d\varphi \sin \theta d\theta}{g^{3/2}(\theta, \varphi)} \approx (0.35 m_0)^{3/2},$$

$$g(\theta, \varphi) = A - [B^2 + C^2 \sin^2 \theta (\sin^2 \theta \sin^2 \varphi \cos^2 \varphi + \cos^2 \theta)]^{1/2}.$$

Some of the results of a numerical simulation of the conductivity $\sigma = \bar{P}/E_1^2$ of p -Ge are shown in Fig. 6. The values of σ at $E_1/E \ll 1$ correspond to a linear conductivity. According to the result of the linear theory, the conductivity reaches a maximum at the cyclotron resonance, $\omega \approx \omega_{c0}$, and at $H = 25$ kOe, $\lambda = 2$ mm, and $N_0 = 10^{14}$ cm⁻³ this conductivity is $\sigma \approx -1.0 \cdot 10^{10}$ s⁻¹ $\alpha = 2\pi\sigma/c\varepsilon_0^{1/2} \approx 0.53$ cm⁻¹. This is about half the value found from the analytic calculations and given above. In a strong alternating field $E_1 \sim (0.3-0.5)E$ we observe an increase in the conductivity in absolute value, evidently due to a dynamic change in the structure of the hole distribution function as a result of their capture to the resonant cone. Because of this capture, the region with a negative differential conductivity expands to fields $E_1 \gtrsim E$. These results can be used to determine the limiting power of millimeter-range radiation which can be achieved through the use of p -Ge in fields $E \parallel H$ as the active element of a generator: $P/V = \sigma(E_1)E_1^2 \approx 100$ W/cm³ with $\lambda = 2$ mm and $N_0 = 10^{14}$ cm⁻³. The corresponding efficiency is $\eta \sim 5 \cdot 10^{-3}$. The maximum power radiated from the surface of the semiconductor can be estimated from $P/S = c\varepsilon_0^{1/2}E_1^2/4\pi \approx 200$ W/cm².

5. EXPERIMENTAL PROCEDURE AND RESULTS

The first studies of the cyclotron resonance of holes with a negative effective mass in germanium were carried out as early as 1958–1960 (Ref. 18). Although the results emerging from those experiments were rather contradictory, these were the first steps along the path that led, a quarter of a century later, to the discovery of an induced emission of hot holes with a negative cyclotron mass in germanium.⁴ Several experimental studies which were carried out over these years added substantially to the picture of the distribution function and conductivity of Ge heavy holes. Measurements by optical methods in the near-IR region in Ref. 12 revealed the appearance of a hole distribution function which was elongated along \mathbf{E} in strong fields at $T = 77$ K: streaming (see also Ref. 24). These results were later supplemented with measurements of the hole drift velocities $v(E)$ by a time-of-flight method.²⁵ Some distinctive features of the dynamics of carriers in an anisotropic zone under conditions of nearly collisionless motion at energies $\varepsilon < \hbar\omega_0$ were discovered in Refs. 26–28 on the basis of the cyclotron resonance of Ge heavy holes in fields with $\mathbf{E} \parallel \mathbf{H}$. Finally, we should also mention Kajita's study,²⁹ which, although for p -Si, revealed a negative Hall effect during streaming in the [111] direction, with negative transverse masses.

5.1 Absorption of electromagnetic radiation in p -Ge in fields with $\mathbf{E} \parallel \mathbf{H}$

An interaction of centimeter-range electromagnetic radiation with holes in germanium in strong electric fields $\mathbf{E} \parallel [001]$ was first studied by Gershenzon *et al.*³⁰ at $T = 77$ K. The results showed that it was not possible to achieve NEMAG in p -Ge at liquid-nitrogen temperature without a magnetic field. In the present experiments, we studied the absorption at $\lambda \sim 2$ mm of p -Ge at liquid-helium temperatures under cyclotron resonance conditions, using the procedure described in Ref. 27. The quantity which was measured directly was the change in the transmission of the linearly polarized radiation from a backward-wave tube under the influence of a pulse of an electric $\mathbf{E} \parallel \mathbf{H} \parallel [001]$. The parallel-plate p -Ge sample was positioned in a quasi-optical section and oriented perpendicular to the wave vector of the radiation. In the absence of an electric field E at $T = 4.2$ K, all the holes in the sample were frozen in shallow acceptor levels, and the sample was transparent to the millimeter-range radiation. The strong electric-field pulse produced ioniza-

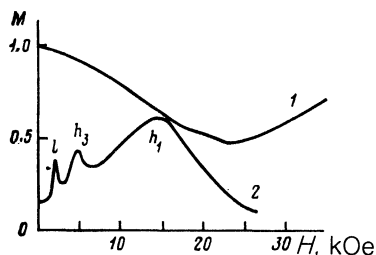


FIG. 7. Modulation of the millimeter-range radiation from a backward-wave tube ($\lambda \sim 2$ mm) by a p -Ge sample versus the magnetic field. 1— $D = 100$ V/cm ($\mathbf{E} \parallel \mathbf{H}$); 2— $E = 0$ ($T \lesssim 10$ K).

tion and then heating of holes. The wavelength of the backward-wave tube was chosen so that the wave propagation path was equal to an integer number of half-wavelengths. In this case, with a slight modulation of the transmission of the sample, $M \ll 1$, the magnitude of the measured signal for optically thin plates was proportional to the real part of the hole conductivity in the electric field. Figure 7 shows the modulation of the transmission as a function of the magnetic field, according to measurements at the time at which pulses of a strong electric field $E = 100$ V/cm were applied to the sample and immediately after these pulses ($E = 0$). In the latter case, the modulation stems from thermal activation of the holes from impurity levels into the valence band as a result of the heating of the crystal during the field pulse. The sample temperature was chosen in such a way that the degree of thermal ionization of the acceptors was low, so that the modulation of the transmission was slight. The line l in the spectrum corresponds to the cyclotron resonance of light holes, while $h_{1,3}$ are the first and third harmonics of the cyclotron resonance of heavy holes.

In a strong field, $E \approx 100$ V/cm, in which essentially all the acceptors are ionized, the sample is transparent to the radiation from the backward-wave tube: $M \approx 1$ at $H = 0$. In a magnetic field with $\mathbf{H} \parallel \mathbf{E}$ we observed an increase in the transmission of the sample to $M \lesssim 0.5$, apparently due to vanishing (or even a change in the sign) of the hole conductivity in an electric field of circular polarization in the electron direction which is in resonance with the cyclotron revolution of holes with a negative cyclotron mass. For the hole direction of the circular polarization of the electric field, the conductivity remained high, so that only one of the two circularly polarized components of the incident plane-polarized wave passed through the sample. The maximum increase in transmission [the minimum of $M(H)$] is found at magnetic fields corresponding to a cyclotron mass $m_c \approx 0.5m_c$, as we would expect for inverted holes with a negative cyclotron mass (Fig. 4).

5.2. Generation of electromagnetic radiation in p -Ge in fields such that $\mathbf{E} \parallel \mathbf{H}$

Figure 8 is a schematic diagram of the apparatus used in the present experiments to observe the stimulated emission. We studied samples of weakly compensated Ge:Ga. The samples were held in a liquid-helium cryostat, at the center of a superconducting solenoid. A voltage pulse applied to the sample through noninjecting contacts ($\tau_p \sim 1-80$ μ s, $f_{\text{rep}} \lesssim 200$ Hz, $E \gtrsim 5$ V/cm), as in experiments on the absorption of electromagnetic radiation, caused impact ionization of shallow impurities and set up a drift of charge carriers along the [001] crystallographic direction. The radiation was detected by an n -InSb detector outside the magnetic field of the solenoid. The pulsed output signal from this detector was amplified, converted into a static voltage by a strobe integrator, and fed to the Y input of an x, y chart recorder. The signal was built up on the strobe integrator over the length of the reference strobe pulse. A slowly varying voltage proportional to the current through the solenoid or to the delay of the strobe pulse was fed to the X input of the

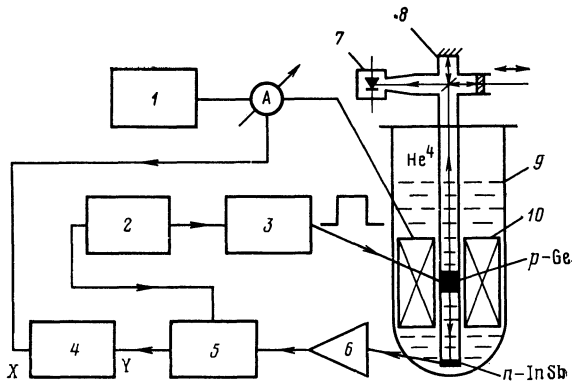


FIG. 8. Block diagram of the apparatus used to study the emission from p -Ge samples in fields, E , H . 1—Power supply for solenoid; 2—trigger pulse generator; 3—generator of the strong electric field pulses; 4— x , y recorder; 5—strobe integrator; 6—broad-band amplifier; 7—Schottky-barrier diode; 8—Michelson interferometer; 9—helium cryostat; 10—superconducting solenoid.

recorder. The recorder thus recorded either the dependence of the emission intensity on the magnetic field or the shape of the emission pulse.

Stimulated emission from p -Ge was observed under conditions similar to those under which the maximum increase in the transmission of the sample was observed. Figure 9 shows some typical results on the behavior of the emission intensity as a function of the magnetic field. The emission arose after a threshold was reached, in the field intervals $E \sim (70-320)$ V/cm, $HG \sim (15-50)$ kOe; its intensity was more than five orders of magnitude higher than that of the spontaneous emission of p -Ge under similar conditions.²² Figure 10 shows the emission zones of several samples. The boundary values of fields E and H were determined by the balance between the resonant amplification, on the one hand, and the nonresonant hole absorption and other loss mechanisms, which do not involve free carriers, on the other. The dependence of the hole conductivity on the magnetic field was found in the preceding section [see (7), (8)]; $\sigma_{\text{res}} \propto 1/H$, $\sigma_h \propto 1/H^2$ at a fixed value of the field E . It

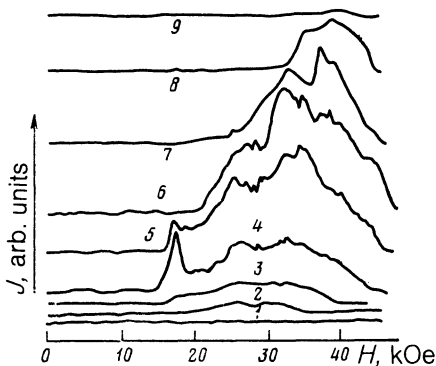


FIG. 9. Intensity of the emission from p -Ge (sample 1) versus the magnetic field in the band of the n -InSb detector at several values of E (V/cm): 1—50; 2—80; 3—90; 4—120; 5—140; 6—195; 7—250; 8—275; 9—310. The curves have been displaced along the ordinate for clarity.

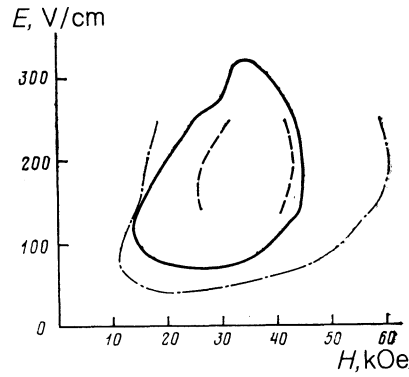


FIG. 10. Emission zones of various p -Ge samples. Solid line—Sample 1; dot-dashed line—sample 2, made from the same material as sample 1, but with twice the length along the direction of H ; dashed line—sample 3, of the same configuration as sample 2, but made from a material with a dopant concentration three times higher.

follows that when there is a large difference between the lower and upper boundary values of H the former will be determined primarily by the balance between σ_{res} and σ_h , while the latter will be determined primarily by the resonant amplification and the other loss mechanisms.

The range of electric fields in which emission is observed corresponds to the maximum anisotropy (an elongation along E) of the distribution function of the Ge heavy holes at $T \sim (5-20)$ K (Ref. 13) and to its localization in the negative-cyclotron-mass cone. At lower electric fields, the time over which a hole must move to reach the energy of an optical phonon is comparable to or shorter than the scale time for scattering by acoustic phonons, so that streaming does not set in. On the other hand, in fields $E > 200$ V/cm the distribution function begins to broaden because of the appearance of holes in the region $\epsilon > \hbar\omega_0$. This circumstance reduces the absolute value of σ_{res} (Fig. 4) and increases $\sigma_h \sim \omega_E/\omega_c^2$ [see (8)]. Experimentally, this behavior is seen as a decrease in the emission intensity at fields $E > 200$ V/cm, to the point at which the emission is cut off at a fixed value of the magnetic field (Fig. 9). The substantial narrowing of the emission zone for a more heavily doped sample, 3 (Fig. 10), is apparently also a consequence of a decrease in the anisotropy of the distribution function and of $|\sigma_{\text{res}}|$ due to an additional scattering of holes by ionized centers.

The anisotropy of the distribution function should also fade with increasing temperature of the semiconductor because of enhancement of the acoustic scattering. Under the experimental conditions, the sample is heated adiabatically during the electric field pulse, and it has cooled off slowly to the temperature of the liquid-helium bath, $T = 4.2$ K, by the time the next pulse arrives. The solid lines in the inset in Fig. 11 show the emission pulses at various initial temperatures T_0 of sample 1. The heating from 4.2 K to T_0 is caused by an electric pulse directly preceding the field pulse during which the emission is observed; the values of T_0 and $T(t)$ are calculated³¹ on the basis of an adiabatic heating of the sample during both pulses. Figure 11 shows the temperature dependence of the emission intensity. These results show that the

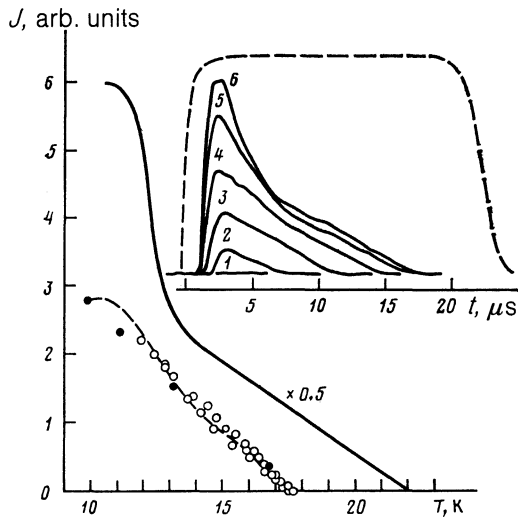


FIG. 11. Temperature dependence of the emission intensity of sample 1 (dashed line) and sample 2 (solid line) at $T_0 = 4.2$ K, $E = 150$ V/cm, and $H = 27$ kOe. ●—Data corresponding to the crests of pulses 2–6 in the inset; ○—data from various regions of pulses 2–5. The inset shows oscilloscope traces of the emission pulses from sample 1 found at various initial lattice temperatures T_0 when the voltage pulse is applied to the sample (dashed line). T_0 (K): 1—17.4; 2—16.8; 3—15.2; 4—13.2; 5—8.5; 6—4.2.

decrease in the emission intensity during the pulse results from an increase in the temperature of the sample; the preliminary heating and the heating during the field pulse affect the emission intensity in identical ways.

The linear behavior of the radiated power P as a function of T near the cutoff temperature (where the generation is cut off; Fig. 11), can be explained by using the balance equation for amplification and absorption in the sample,

$$\sigma_{\text{res}} + \sigma_h + \sigma_l = 0, \quad (13)$$

and the resonant conductivity approximation

$$\sigma_{\text{res}} = -\sigma^* (1 - \beta E_1^2) (1 - \gamma T), \quad (14)$$

in the region where σ_{res} deviates very slightly from linear conductivity (see the curve in Fig. 5 for $\lambda = 2$ mm and $H = 34$ kOe at fields $E_1 \ll E$). Here σ_l is the effective conductivity, which incorporates all types of loss. The quadratic field term in (14) arises from the iteration following (6) in the small parameter $E_1/E \ll 1$ in the kinetic equation. The temperature factor $\gamma T \ll 1$ is related to the decrease in the number of holes which are involved in the streaming and which contribute to σ_{res} because of scattering by acoustic phonons: $v_{\text{ac}} \sim T E^{1/2}$. Accordingly, under conditions near the cutoff of the generation, we find from (13) and (14)

$$P \propto E_1^2 \propto \left(1 - \frac{\sigma_h + \sigma_l}{\sigma^*}\right) - \frac{\sigma_h + \sigma_l}{\sigma^*} \gamma T;$$

i.e., that radiation power falls off in proportion to the temperature (Fig. 11). The apparent reason for the deviation of $P(T)$ from linearity for the longer sample 2 (for which the emission zone is broader, as can be seen from Fig. 10, so that the value of σ_l is smaller) at $T < 13$ K is the autoresonant behavior of the holes in the strong alternating field E_1 , in

which the behavior $\sigma_{\text{res}} \propto (1 - \beta E_1^2)$ is disrupted (Section 4).

The question of the limiting temperatures for the existence of a negative differential conductivity in p -Ge requires additional study, but some qualitative conclusions can be drawn from even the results presently available. The effect of the temperature on the resonant conductivity can be estimated from (14), which, as we have shown, gives a satisfactory description of the experimental results found at $T < 20$ K. As was mentioned above, the temperature factor in (14) results from the acoustic scattering of holes over the transit time ω_E^{-1} : $\gamma T = \bar{v}_{\text{ac}} / \omega_E$, where \bar{v}_{ac} is the average of $1.07 \cdot 10^8 T [\text{K}] (\epsilon / k_B [\text{K}])^{1/2} [\text{s}^{-1}]$. An estimate of \bar{v}_{ac} for the simplest, needle-shaped, streaming model yields $\gamma T + 1.4 T [\text{K}] / E [\text{V/cm}]$, or $\gamma T = 0.14$ with $T = 20$ K and $E = 100$ V/cm. The factor γT remains small if the field E increases with increasing T . At $T \sim 80$ K we have $\gamma T \lesssim 0.2$ at $E \gtrsim 600$ V/cm, and if the conductivity σ_{res} were negative at liquid-helium temperatures in such fields the conductivity would retain its sign at $T = 80$ K. We have not made a detailed study here of the possibility of lasing in such strong fields. Lasing was observed, however, at liquid-helium temperatures in comparatively weak fields, $E \sim 40$ – 50 V/cm, which correspond, according to Ref. 13, to the same degree of anisotropy of the distribution and thus the same value of σ_{res} as do fields $E \sim 600$ V/cm. As E is increased from 50 to 600 V/cm, there will of course be an increase in the loss associated with the contribution to the conductivity of the uninverted part of the distribution function, σ_h , but the relation between σ_{res} and σ_h can be improved by increasing the magnetic field [see (7) and (8)]. We thus see that a negative differential conductivity at the cyclotron resonance of heavy holes in Ge in fields with $E \parallel H$ can be reached at temperatures substantially above 20 K, but the interval along the magnetic-field scale in which the generation occurs will become narrower with increasing temperature.

Spectral studies of the induced emission were carried out with a Michelson interferometer (Fig. 8) and also with a superheterodyne receiver outside the cryostat. The emission

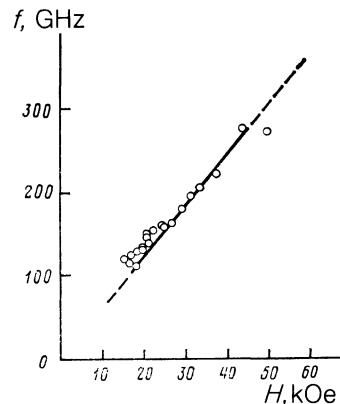


FIG. 12. Tuning the output frequency of the maser with a magnetic field. The dashed lines are the limiting values of the magnetic field at which emission was found in sample 2.

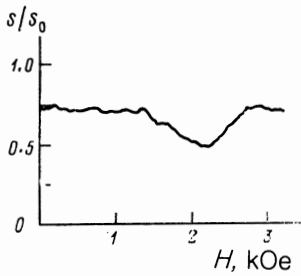


FIG. 13. Cyclotron resonance in p -Ge in fields $\mathbf{E} \perp \mathbf{H}$ ($E \sim 50$ V/cm). Here S_0 is the signal level at the receiver in the absence of an electric field at the sample.

from the sample reached the receiver and the interferometer along an oversized metal waveguide. Schottky-barrier diodes were used as rectifier and mixer. The signal is a rather narrow spectral line, with a width which is, less than or equal to the spectral resolution of the interferometer and of the superheterodyne receiver (60 and 40 MHz, respectively). Figure 12 shows the emission frequencies found with the help of the interferometer, along with the approximation $f(H)$ in the interval of magnetic fields in which the emission is observed. The experimental points conform satisfactorily to the line, which corresponds to the functional dependence $f = (eH/m^*c)/2\pi$ with an effective mass $m^* \approx 0.45m_0$. The results shown here were obtained for various values of E ; within the measurement error, we observed no dependence of the emission frequency on the electric field. The change in the frequency with the magnetic field stems from a change in the structure of the gain band and a competition among modes in the generator, with the result that induced emission is established at the frequency of the mode having the highest linear growth rate.

Since the emission from this semiconductor maser is highly monochromatic, it can be used for spectral studies. A first experiment along this line involved the observation of the cyclotron resonance of light holes in germanium in fields $\mathbf{E} \perp \mathbf{H}$. The semiconductor generator and the test sample were placed in superconducting solenoids in different cryostats. The emission from the generator, with a wavelength $\lambda \approx 1.9$ mm, was channeled through an oversized section holding the p -Ge sample, and it was detected by a cooled n :InSb detector. The measurement procedure here was analogous to that used in the experiments on the absorption in p -Ge in fields $\mathbf{E} \parallel \mathbf{H}$ (Subsection 5.1). A pulsed electric field $E \sim 50$ V/cm, which ionized shallow acceptor impurities and then heated the holes, was applied to the sample in synchronization with the generator pulses. The result was to attenuate the signal, by virtue of the absorption of the emission by free carriers (Fig. 13). As the magnetic field at the sample was varied, we observed the cyclotron-resonance line of light holes in Ge (Fig. 13; cf. Refs. 26 and 27). This experiment demonstrates the use of a semiconductor generator for the spectroscopy of hot carriers, although the possibilities here are much broader and stem primarily from the broad range over which the wavelength can be tuned.

CONCLUSION

The results of this experimental study of the emission from p -Ge in fields $\mathbf{E} \parallel \mathbf{H}$, i.e., the conditions under which emission is observed, the threshold required for the onset of emission, the suppression by heating the crystal, and the fact that the output wavelength can be tuned by means of a magnetic field, leave no doubt that stimulated emission has been achieved in a maser which operates by virtue of the cyclotron resonance of holes with negative effective masses: cyclotron-resonance NEMAG. Like other new sources of radiation in the submillimeter¹⁻³ and millimeter⁵ ranges, NEMAG has so far been implemented only in comparatively pure germanium at liquid-helium temperatures.⁹ Moving to substantially higher temperatures will require improving the design of the apparatus and using other materials. The materials of primary interest for NEMAG are silicon and diamond of p -type conductivity. The energy of an optical phonon in these semiconductors is two to four times larger than that in germanium, so that we could expect a rather narrow distribution function during streaming in an electric field, not only at liquid-helium temperatures but also at higher temperatures. Furthermore, the minimum values of the negative effective mass for holes at the axis of the negative-cyclotron-mass cone in these materials are three to seven times smaller than in p -Ge, so that emission can be achieved in weaker magnetic fields. These properties are of course only prerequisites which qualify these materials as promising. Final conclusions will have to await a detailed study of the conductivity, like that which has been carried out for p -Ge. For diamond and silicon, an important property along the anisotropy of the dispersion law is that its dispersion law is not parallel (the energy of the spin-orbit splitting of these materials is lower than the energy of an optical phonon), so that a rigorous consideration of all features of the scattering and dynamics of holes becomes a complicated problem even for a Monte Carlo numerical simulation.

Also of interest would be a study of the possibilities of a negative conductivity at cyclotron resonance in polar p -type semiconductors, e.g., p -GaAs. In these materials, because of the predominant small-angle scattering in interactions with optical phonons, conditions are more favorable for localization of the distribution function in the negative-cyclotron-mass cone. We believe that the future development of both experimental and theoretical research on the cyclotron resonance of holes with a negative effective mass will add substantially to our understanding of the possibilities of semiconductor cyclotron-resonance masers.

We wish to thank Yu. A. Dryagin, L. M. Kukin, and V. V. Parshin for assistance in the studies of the spectral characteristics of the emission.

¹Analysis of the dispersion law shows that similar cones also exist along [111] axes. In the valence band of germanium, these cones lie at energies above the energy of an optical phonon, $\epsilon > \hbar\omega_0$, and they are of no interest here, for reasons that we will give below.

²This value agrees with an estimate found for the limit $\omega \rightarrow 0$ in Ref. 13.

³There is the possibility that at $T > 30$ K a negative differential conductivity would be attainable in thin films of a p -type semiconductor, where the conditions for the occurrence of an inversion might be more favorable.¹⁵⁻¹⁷

- ⁴Under the condition $\omega_c \gg \omega_E, \nu$, the shape of the cyclotron-resonance line of germanium heavy holes with a negative cyclotron mass is determined by the dispersion of the cyclotron frequencies, $\omega_c(S, p_z)$, and by the static distribution function $f_0(E, H)$.
- ⁵A capture also occurs in a linearly polarized field E_1 if resonant conditions are satisfied for one of the two circularly polarized components of the wave.
- ⁶The average is taken over long time intervals, during which a hole experiences tens of thousands of scattering events.
- ⁷Here and below, the numerical values of the parameters are given for p -Ge.
- ⁸This approximation holds in p -Ge under streaming conditions at $T \gtrsim 12$ K. At lower temperatures, it becomes necessary to resort to the approximation of zero-point lattice vibrations.
- ⁹Vorob'ev *et al.*¹ also reported observing an emission at $T \approx 80$ K in p -Ge in fields EH in the range $\lambda \sim 100 \mu\text{m}$.
- ¹L. E. Vorob'ev, F. I. Osokin, V. I. Stafeev, and V. N. Tulupenko, *Pis'ma Zh. Eksp. Teor. Fiz.* **3**, 360 (1982) [*JETP Lett.* **35**, 440 (1982)].
- ²Yu. L. Ivanov and Yu. V. Vasil'ev, *Pis'ma Zh. Tekh. Fiz.* **9**, 613 (1983); **10**, 949 (1984) [*Sov. Tech. Phys. Lett.* **9**, 264 (1983); **10**, 398 (1984)].
- ³A. A. Andronov, I. V. Zverev, V. A. Kozlov, *et al.*, *Pis'ma Zh. Eksp. Teor. Fiz.* **40**, 69 (1984) [*JETP Lett.* **40**, 804 (1984)].
- ⁴A. A. Andronov, A. M. Velyantsev, V. I. Gavrilenko, *et al.*, *Pis'ma Zh. Eksp. Teor. Fiz.* **40**, 221 (1984) [*JETP Lett.* **40**, 989 (1984)].
- ⁵A. P. Chebotarev and V. A. Murzin, *Pis'ma Zh. Eksp. Teor. Fiz.* **40**, 234 (1984) [*JETP Lett.* **40**, 1005 (1984)].
- ⁶H. Krömer, *Phys. Rev.* **109**, 1856 (1958); *Proc. IRE* **47**, 397 (1959); *Prog. in Semicond.*, Vol. 4, London, 1960, p. 3.
- ⁷A. A. Andronov, in: *Invertirovannye raspredeleniya goryachikh elektronov v poluprovodnikakh* (Population Inversions of Hot Electrons in Semiconductors), Gor'kiï, 1983, p. 5.
- ⁸N. G. Basov, O. N. Krokhin, and Yu. M. Popov, *Zh. Eksp. Teor. Fiz.* **38**, 1001 (1960) [*Sov. Phys. JETP* **11**, 720 (1960)]; *Usp. Fiz. Nauk* **72**, 164 (1960) [*Sov. Phys. Usp.* **3**, 702 (1961)].
- ⁹Yu. Kogan, *Zh. Eksp. Teor. Fiz.* **38**, 1854 (1960) [*Sov. Phys. JETP* **11**, 1333 (1960)].
- ¹⁰I. M. Tsidil'kovskii, *Elektrony i dyrki v poluprovodnikakh* (Electrons and Holes in Semiconductors), Nauka, Moscow, 1972, §§14, 30.
- ¹¹YU. V. Gulyaev and I. I. Chusov, *Fiz. Tverd. Tela* (Leningrad) **21**, 2637 (1979) [*Sov. Phys. Solid State* **21**, 1517 (1979)].
- ¹²W. E. Pinson and R. Bray, *Phys. Rev.* **136**, 1449 (1964).
- ¹³T. Kurosawa and H. Maeda, *J. Phys. Soc. Jpn.* **31**, 668 (1971).
- ¹⁴C. Jacabini and L. Reggiani, *Rev. Mod. Phys.* **55**, 645 (1983).
- ¹⁵F. Herman, European patent specification 0031452B1, Int. Cl. HOIL 47/00, 1980.
- ¹⁶Yu. K. Pozhela, *Fiz. Tekh. Poluprovodn.* **18**, 1467 (1984) [*Sov. Phys. Semicond.* **18**, 916 (1984)].
- ¹⁷Yu. K. Pozhela, E. V. Starikov, and P. N. Shiktorov, Proceedings of the Fourth International Conference on Hot Carrier Semiconductors, Innsbruck, 1985.
- ¹⁸G. C. Dousmanis, *Phys. Rev. Lett.* **1**, 55, 168 (1958); G. C. Dousmanis, R. C. Duncan, J. J. Thomas, and R. C. Williams, International Conference on Semiconductor Physics, Prague, 1960, p. 603.
- ¹⁹A. A. Andronov, V. I. Gavrilenko, E. P. Dodin, Z. F. Krasil'nik, and M. D. Chernobrovcheva, Preprint No. 40, Institute of Applied Physics, Gor'kiï, 1981.
- ²⁰R. C. Williams and F. Herman, Proceedings of the International Conference on Semiconductor Physics, Prague, 1960, p. 599.
- ²¹A. A. Andronov, E. P. Dodin, and Z. F. Krasil'nik, *Fiz. Tekh. Poluprovodn.* **16**, 212 (1982) [*Sov. Phys. Semicond.* **16**, 133 (1982)].
- ²²L. V. Berman, V. I. Gavrilenko, Z. F. Krasil'nik, *et al.*, *Fiz. Tekh. Poluprovodn.* **19**, 369 (1985) [*Sov. Phys. Semicond.* **19**, 231 (1985)].
- ²³E. P. Dodin and Z. F. Krasil'nik, *Fiz. Tekh. Poluprovodn.* **18**, 944 (1984) [*Sov. Phys. Semicond.* **18**, 588 (1984)].
- ²⁴L. E. Vorob'ev, Yu. K. Pozhela, A. S. Reklaitis, *et al.*, *Fiz. Tekh. Poluprovodn.* **12**, 742-754 (1978) [*Sov. Phys. Semicond.* **12**, 443, 440 (1978)].
- ²⁵L. Reggiani, C. Canali, F. Nava, and G. Ottaviani, *Phys. Rev.* **B16**, 2781 (1977).
- ²⁶V. I. Gavrilenko, E. P. Dodin, Z. F. Krasil'nik, Yu. N. Nozdrin, and M. D. Chernobrovcheva, *Pis'ma Zh. Eksp. Teor. Fiz.* **35**, 432 (1982) [*JETP Lett.* **35**, 535 (1982)].
- ²⁷V. I. Gavrilenko, E. P. Dodin, and Z. F. Krasil'nik, in: *Invertirovannye raspredeleniya goryachikh elektronov v poluprovodnikakh* (Population Inversions of Hot Electrons in Semiconductors), Gor'kiï, 1983, p. 141.
- ²⁸A. A. Andronov, V. I. Gavrilenko, O. F. Grishin, *et al.*, Proceedings of the Fifth Symposium on Plasmas and Instabilities in Semiconductors, Vil'nyus, 1983, p. 82.
- ²⁹K. Kajita, *Solid State Commun.* **31**, 573 (1979).
- ³⁰E. M. Gershenzon, Yu. A. Gurevich, and L. B. Litvak-Gorskaya, *Ukr. Fiz. Zh.* **9**, 948 (1964).
- ³¹P. Flubacher, A. J. Leadbetter, and J. A. Morrison, *Philos. Mag.* **4**, 273 (1959).

Translated by Dave Parsons